MITSUBISHI ELECTRIC RESEARCH LABORATORIES
https://www.merl.com

Analytical Green's functions for two-dimensional electrostatics and Boundary-element based solver

Lin, Chungwei; Wang, Bingnan

TR2024-060 May 25, 2024

Abstract

We derive analytical Green's functions for two- dimensional (2D) electrostatic problem, based on which a boundary-element based 2D electrostatic solver is developed. The system is composed of perfect electric conductors and linear dielectric materials; the boundary conditions are specified by an applied field and the total charge of each conductor. The solver is benchmarked by computing the macroscopic parameter of the system and comparing them to the exact values. Two applications are considered. First we determine the characteristic impedance of a microstrip transmission line; the results agree well with established values in literature. Second we compute the sensitivity of the field-induced torque with respect to the shape deformation. The consistent results using the finite difference and the adjoint method indicates that our solver is sufficiently precise to reliably tell the difference between two very similar shapes.

Applied Computational Electromagnetics Society Symposium (ACES) 2024

Mitsubishi Electric Research Laboratories, Inc.
201 Broadway, Cambridge, Massachusetts 02139

***Abstract*—We derive analytical Green's functions for two-dimensional (2D) electrostatic problem, based on which a boundary-element based 2D electrostatic solver is developed. The system is composed of perfect electric conductors and linear dielectric materials; the boundary conditions are specified by an applied field and the total charge of each conductor. The solver is benchmarked by computing the macroscopic parameter of the system and comparing them to the exact values. Two applications are considered. First we determine the characteristic impedance of a microstrip transmission line; the results agree well with established values in literature. Second we compute the sensitivity of the field-induced torque with respect to the shape deformation. The consistent results using the finite difference and the adjoint method indicates that our solver is sufficiently precise to reliably tell the difference between two very similar shapes.**

***Index Terms*—electrostatic solver, complex analysis, transmission line**

Analytical Green's functions for two-dimensional electrostatics and Boundary-element based solver

Chungwei Lin and Bingnan Wang Mitsubishi Electric Research Laboratories, 201 Broadway, Cambridge, MA 02139, USA,
clin@merl.com and bwang@merl.com

I. Introduction

Two-dimensional electrostatic/megnetostatic problems are usually the first approximation to describe the realistic problems. Built upon the complex analysis done in Refs. [1], [2] we identify the analytical expressions for potential and dyadic Green's functions for 2D electrostatic problem. We then develop a boundary-element (BEM) based potential and field solver to describe systems composed of perfect conductors (metal) and dielectric materials in an external field. We shall use $\mathbf{X} = (X, Y)$ ($\mathbf{x} = (x, y)$) or $Z = X + jY$ ($z = x + jy$) to represent a 2D position in this work.

II. Analytical Green's function and solver

We derive the closed-form potential Green's function:

$$
\begin{aligned}
&G_P(Z|z_2, z_1) \\
=&\frac{2|z_2 - z_1|}{z_2 - z_1}\Bigg[\left(Z - \frac{z_1 + z_2}{2}\right) \cdot \log\left(\frac{z_2 - Z}{z_1 - Z}\right) \\
&- \frac{z_2 - z_1}{2}\log\left[(z_2 - Z)(z_1 - Z)\right] + (z_2 - z_1)\Bigg].
\end{aligned} \quad (1)
$$

Namely, given a uniform charge density λ between z_1 and z_2, the resulting electrostatic potential (satisfying $-\nabla^2 V = 4\pi\lambda$) at Z is $\lambda \mathrm{Re}[G_P(Z|z_1, z_2)]$. Analytical dyadic Green's functions can be obtained by taking Z derivative.

Consider a metal surface specified by boundary points $\{z_0, \cdots z_N\}$ and the ith element between $[z_{i-1}, z_i]$ carrying a charge λ_i ($i = 1$ to N), the induced potential at Z by boundary charges is given by $\Phi_{\text{ind}} = \sum_{i=1}^{N} \lambda_i G_P(Z|z_i, z_{i-1})$. Given an external potential Φ_{ext} the charge distribution $\{\lambda_i\}$ can be determined by minimizing the electrostatic energy

$$
E_{\text{ele}} = \frac{1}{2}\int \mathbf{dx}\, \rho(\mathbf{x})\Phi_{\text{ind}}(\mathbf{x}) + \int \mathbf{dx}\, \rho(\mathbf{x})\Phi_{\text{ext}}(\mathbf{x}), \quad (2)
$$

subject to a specified total charge $\sum_i \lambda_i |z_i - z_{i-1}| = Q$. We use Quadratic-Programming to get $\{\lambda_i\}$; once $\{\lambda_i\}$ is known, the fields can be accurately evaluated using Green's functions. Eq. (1) can be applied to point-matched Method of Moment [3]. We generalize our solver to include both metals and dielectric materials utilizing the analytical dyadic Green's functions.

Our solver determines the distributed capacitance by the following setup: assigning charges ± 1 to two metals and computing their potential difference $|\Delta V|$, the distributed capacitance C_{solver} is evaluated by

$$
C_{\text{solver}} = \frac{4\pi\varepsilon_0}{|\Delta V|} \equiv \varepsilon_0 \mathcal{C}_{\text{solver}}. \quad (3)
$$

$\mathcal{C}_{\text{solver}}$ is the normalized capacitance. Eq. (3) will be used for determining the transmission line (TL) parameters.

III. Benchmarks and Applications

Two applications will be considered. The first one is to compute the characteristic impedance Z_c of a microstrip TL. In the low-frequency limit, the EM field of a TL can be approximated by a TEM mode and the problem is reduced to the electrostatics [4]. Determination of Z_c in the electrostatic approximation requires two calculations. The first one is the configuration without dielectric materials, and the resulting distributed capacitance C_{vac} is used to determine the distributed inductance L. The second calculation is for the actual configuration from which we get the distributed capacitance C. The characteristic impedance is given by

$$
Z_c = \sqrt{\frac{L}{C}} = \frac{120\pi}{(\mathcal{C}_{\text{vac}}\mathcal{C})^{1/2}} \text{ (Ohm)}. \quad (4)
$$

Here $\mathcal{C} = C/\varepsilon_0$ is the normalized distributed capacitance.

As a concrete example we compute Z_c for a microstrip TL considered in Chapter 4 of Ref. [5]. The configuration is indicated in Fig. 1(b). GaAs of $\varepsilon_r = 12.9$ is filled between the metal strip and ground plane. To determine Z_c, the first step is to compute C without dielectric filling; this problem can be solved using Conformal Mapping technique and resulting C's are tabulated in p.896 of Ref. [5]. Fig. 1(a) shows the results from our solver and those from Conformal Mapping; a very agreement is seen.

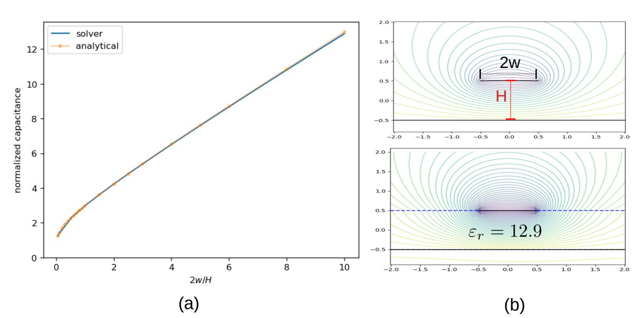

FIG. 1: (a) Normalized capacitance for a microstrip line of width $2w$ at a height of H above the ground plane. The results from our solver agree well with those from Conformal Mapping method tabulated in Ref. [4]. The ground plane of a width of 20 is used. (b) Computed equipotentials for $2w = 1$ and $H = 1$. (Top) No dielectric is filled between the microstrip line and ground plane. (Bottom) GaAs of $\varepsilon_r = 12.9$ is filled. The computed Z_c's are given in Table I.

The computed Z_c's using Eq. (4) are summarized in Table I; the solver for dielectric materials is used (not described here). The relative errors between our method and literature values

$Z_{c,\text{lit}}$ given in Fig.(4.28) in Ref. [5] are smaller than 3%, which is very reasonable considering the slightly different boundary conditions used in Ref. [5]. The configurations and selected equipotentials with and without GaAs are shown in Fig. 1(b). In our calculations the ground metal plane has a width of 10 and a tiny gap of 10^{-3} between the metal segments and the dielectric.

$2w/H$	0.25	0.5	1.0	2.0	4.0
$Z_{c,\text{lit}}$	74.5	58.5	43.2	29.6	18.4
$Z_{c,\text{solver}}$	73.556	60.088	44.317	30.125	18.801
C	14.642	17.5934	24.568	37.586	63.123
err (%)	1.3	2.7	2.6	1.8	2.2

TABLE I: Z_c (in Ohm) of a stripline of width $2w$. Relative error err is $|Z_{c,\text{solver}} - Z_{c,\text{lit}}|/Z_{c,\text{lit}}$.

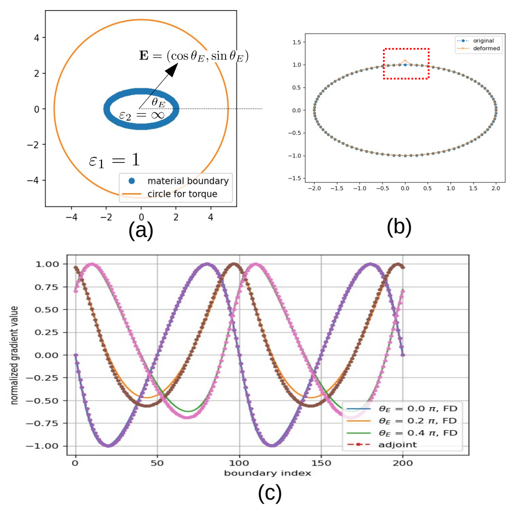

FIG. 2: Shape optimization for maximum torque. The setup is a perfect metal in an external electric field. (a) Configuration of interest. Inside the material boundary $\epsilon_2 = \infty$; outside $\epsilon_1 = 1$. The torque is computed using Eq. (5) that requires the total E-field at the circle. (b) Two material boundaries for evaluating gradient using finite difference; the red box highlights the only difference. (c) Gradient/sensitivity (normalized to one) as a function of boundary index for external fields of different orientations. The adjoint-method and the finite-difference calculations match very well.

The second application is to determine shape sensitivity of the field-generated torque. We consider the simple configuration where a elliptical metal is placed in an external electric field [Fig. 2(a)]; the induced charges on the metal interact with the external field and thus generates a torque. The goal is to compute the gradient of the torque with respect to the shape deformation.

Two essential ingredients are (i) a formula to compute the torque τ; (ii) a description the shape and its deformation. The most convenient way to determine τ is to choose a circle of radius R that encloses the object of interest and then evaluate the stress-tensor to get the torque. Up to a prefactor T_0 the torque τ is given by

$$\tau = T_0 \int_0^{2\pi} d\theta \, E_n(R,\theta) \cdot E_t(R,\theta) \qquad (5)$$

Here θ is polar angle of the circle whose normal and tangential unit vectors are $\hat{n} = (\cos\theta, \sin\theta)$, $\hat{t} = (-\sin\theta, \cos\theta)$.

The object of interest is a metal ellipse whose boundary points $\{z_i\}$ are given by $z_i = 2\cos\theta_i + i\sin\theta_i$ where $\theta_i = (i-1)\cdot\Delta\theta$ with $\Delta\theta = \frac{2\pi}{N}$ and $i = 1$ to N. The *deformation* of the shape is parameterized by the vector $\vec{v} = (v_1, \cdots, v_N)$ where v_i is the displacement of z_i along its normal direction.

The shape sensitivity, defined as $\frac{\partial\tau}{\partial\vec{v}}$, can be evaluated using the finite-difference (FD) approximation or the adjoint method [6]. The former is straightforward both time consuming; the latter requires some derivations but is very efficient. Fig. 2(c) shows that $\frac{\partial\tau}{\partial v_i}$ using adjoint and FD methods match very well for several orientations of external field. It indicates that our solver is capable of capturing the tiny difference between almost-identical shapes with very moderate computational resources. Using FEM to tell the torque difference in Fig. 2(b) may demand a unreasonably fine mesh.

IV. Conclusion

With the analytical expressions provided in this work, the accuracy and efficiency of the 2D BEM-based solver can be significantly improved. Although electrotatics and magnetostatics rarely describe realistic systems, they are good approximations for some tasks as illustrated in our examples. We hope our solver will play a role complementary to that of existing computational methods.

References

[1] R. A. Beth, "Complex representation and computation of two-dimensional magnetic fields," *Journal of Applied Physics*, vol. 37, p. 2568, 1966.

[2] R. A. Beth, "An integral formula for two-dimensional fields," *Journal of Applied Physics*, vol. 38, p. 4689, 1967.

[3] R. F. Harrington, *Field Computations by Moment Methods*. Wiley-IEEE Press, 1993.

[4] R. E. Collin, *Foundations for Microwave Engineering*, 2nd ed. Wiley-IEEE Press, 2001.

[5] Collin, Robert E., *Field theory of guided waves*, 2nd ed. IEEE Press, 1991.

[6] I. H. Park, "Design sensitivity analysis and optimization of electromagnetic systems," *Mathematical and Analytical Techniques with Applications to Engineering*, 2019.